Mon. Not. R. astr. Soc. (1972) **157**, 121–145.

THE EVOLUTION OF SPHERICAL PROTOSTARS WITH MASSES 0·25 $M_\odot$ TO 10 $M_\odot$

Richard B. Larson

(Received 1972 January 17)

SUMMARY

The calculations reported in Paper I for the collapse of a spherical protostar have been improved and extended to a wider range of masses with calculations for masses of 0·25, 0·5, 1·0, 1·5, 2·0, 3·0, 5·0 and 10 solar masses. The method and the assumptions used are similar to those of Paper I except that a better approximation for the temperature distribution in the collapsing protostellar envelope has been incorporated. For masses less than $\sim 1{\cdot}5\ M_\odot$ the results are similar to those obtained previously for a protostar of $1{\cdot}0\ M_\odot$, and they show that a star in this mass range first appears near the lower end of its Hayashi track. For masses greater than $\sim 1{\cdot}5\ M_\odot$ the entropy and the radius of the star never become large enough for a 'Hayashi' phase to exist, and the star first appears on the radiative pre-main sequence track. For masses greater than $\sim 3\ M_\odot$, the central stellar core evolves all the way to the main sequence before beginning to shine through its surrounding cloud; thus no 'normal' pre-main sequence stars should be observed with masses much greater than $\sim 3\ M_\odot$.

The model calculations have been compared with most of the observations thought to relate to star formation or newly-formed stars, with the following results: (1) The early stages of the present protostar models resemble closely some of the dark globules discussed by Bok and others. (2) The infra-red sources in the Orion nebula appear to be best interpreted as protostars of various masses. (3) The observed properties of T Tauri stars and similar objects with dense circumstellar nebulosity are in general agreement with the predicted properties of newly formed stars. (4) The distribution of the pre-main sequence stars of young clusters in the HR diagram is consistent with theoretical expectations based on the present models. Several sources of scatter, including an age spread of $\approx 10^7$ yr, are probably present. (5) FU Ori and V1057 Cyg may be explainable as a result of the rapid dissipation of a protostellar shell by radiation pressure or a stellar wind.

1. INTRODUCTION

In a previous paper (Larson 1969a, hereafter called Paper I) we have described some calculations for the collapse of a spherical protostar of one solar mass, made with a number of different assumptions for the initial and boundary conditions for the collapsing cloud. These calculations explored the effects of variations in the initial temperature, density, and composition of the cloud; a few calculations for larger masses were also tried. The results showed that the qualitative behaviour of a collapsing cloud is always much the same in all cases, regardless of the assumptions made; the collapse is always extremely non-homologous, and leads to the formation of a small stellar core or 'embryo star', which then continues to grow in mass through accretion of the remaining protostellar material. The quantitative results are, of course, somewhat dependent on the assumed conditions, particularly

the initial density of the protostellar cloud; the higher the density, the shorter is the collapse time and the more luminous the resulting star.

In Paper I calculations were also made for masses of 2 and 5 $M_\odot$; the main purpose of these calculations, however, was to find out whether the evolution of a protostar is qualitatively different for different masses, and the assumptions were not chosen in a completely systematic way for all masses. One aim of the present project has been to extend the collapse calculations to a wider mass range, with more systematic and hopefully more realistic assumptions for the initial conditions. With a set of model calculations covering a sufficient range of masses, one should be in a better position to interpret theoretically the properties of objects thought to be protostars or newly formed stars, as well as the HR diagrams of very young clusters. A second aim of this project has been to correct the principal inaccuracy in the calculations of Paper I by improving the treatment of radiative transfer in the infalling protostellar envelope so as to obtain more realistic temperatures in this region.

2. ASSUMPTIONS

The calculations of Paper I were mostly made with an initial temperature of 10°K, but the possibility of an initial temperature as high as 100°K was also considered. The assumed initial temperature is important in that it determines, through the Jeans criterion, the density at which gravitational collapse can begin for a condensation of given mass. Recently, considerable observational evidence has accumulated in favour of low temperatures in the dense dark clouds in which star formation is thought to occur; according to Heiles (1971), the temperatures in such clouds are generally less than 30°K and range down to 5°K or less, a typical value being $\sim$10°K. Theoretical calculations agree in predicting temperatures of the order of 20°K or less for the densest clouds, i.e. those with densities greater than $\sim 10^2$ atoms cm^{-3} (Field 1970). Since the density which a protostar must have in order to collapse is greater than 10^2 atoms cm^{-3}, it appears that one can assume with reasonable confidence that the initial temperature of a collapsing protostar is of the order of 10°K, and probably not greater than 20°K. Accordingly, we have assumed an initial temperature of 10°K in all of the present calculations, except for the largest masses (lowest densities), where a temperature of 20°K has been assumed.

The same assumptions have been made as in Paper I concerning the composition and opacity of the protostellar material; thus the hydrogen is assumed to be all in molecular form, and the infra-red opacity due to dust grains is assumed to have a constant value of 0·15 cm^2 g^{-1}. Also, we have assumed that the collapsing cloud starts from rest with a uniform density distribution, and that it has a radius given by the Jeans criterion in the form

$$R = 0{\cdot}41 \frac{GM}{\mathscr{R}T}. \qquad (1)$$

The boundary of the cloud has been assumed to remain fixed in space as the interior of the cloud collapses. In reality, both the initial conditions and the boundary conditions for a collapsing protostar are rather uncertain, since the initial conditions depend on the previous history of the material, and the boundary conditions depend on the properties of the surrounding interstellar matter. It is conceivable, for example, that under different circumstances the boundary of the cloud might

either contract or expand with time; as a compromise between these extreme possibilities, we have assumed that the boundary remains stationary. Uncertainties in the initial and boundary conditions should not greatly affect the qualitative behaviour of a collapsing cloud (see, for example, Bodenheimer & Sweigart 1968), but they can produce a significant dispersion in the properties of newly formed stars (see Section 5 and 6).

A further uncertainty is introduced by the effects of rotation and/or deviations from spherical symmetry on the collapse of a protostar. From the calculations of Larson (1972), it appears that in most cases deviations from spherical symmetry will not be very important for the collapse, and that the outcome will be much the same as for the spherical case. For a rotating cloud, however, the calculations show that the cloud will not collapse into a single star but will instead fragment into two or more condensations orbiting around the centre; presumably the final outcome of the collapse will be the formation of a multiple system of stars orbiting around each other. It seems likely that each of these stars will form by a process analogous to that found in the spherical case, i.e. non-homologous collapse leading to the formation of a stellar core which then continues to grow by accretion. If so, the spherical collapse calculations should still retain some usefulness as a limiting case whose results are qualitatively valid and quantitatively not in error by many orders of magnitude. Again, however, the effects of rotation may be expected to produce a significant dispersion in the results.

3. THE TEMPERATURE DISTRIBUTION IN THE INFALLING CLOUD

The present calculations have been made using essentially the same method as in Paper I, the main difference being in the use of an improved approximation for treating the transfer of radiation in the collapsing cloud. In Paper I the radiative diffusion equation was used throughout the calculations to describe radiative transfer in the cloud, even though it is physically valid only at large optical depths; when applied in optically thin regions, this equation yields temperatures which are too low during the later stages of the collapse. In the present investigation we have used the same procedure which was used earlier for calculating the emitted spectrum of a collapsing protostar (Larson 1969b, hereafter called Paper II).

The procedure used in Paper II for approximating the temperature distribution in the infalling cloud consisted of adding together the expressions for T^4 applying in the limits of large and small optical depths. The resulting formula gives the correct temperatures in these two limits and provides a smooth transition in between. In the special case of a grey opacity, this simple procedure gives results which are surprisingly accurate (errors less than 13 per cent in T^4 or 3 per cent in T) when compared with detailed solutions computed by Hummer & Rybicki (1971). As we show below, in the grey case this approximation can be formulated as a modification to the diffusion equation which is readily incorporated into the dynamical calculations. In reality the infra-red absorption coefficient for the dust grains is almost certainly non-grey; however, since the infra-red absorption coefficient of the dust grains is still quite poorly known, and since it would be rather more complicated to treat the non-grey case, we have considered it adequate for the present to use the grey approximation, and we have assumed a constant grey opacity of $0{\cdot}15$ cm^2 g^{-1} as before.

To apply the procedure outlined above, we first write the expressions for T^4

which hold in the optically thick and optically thin limits. In the optically thick case, radiative transfer is described by the diffusion equation:

$$L = -\frac{64\pi\sigma r^2 T^3}{3\kappa\rho}\frac{dT}{dr}. \tag{2}$$

Rewriting this equation to give an expression for T^4, we have

$$T^4 = -\frac{3\kappa\rho TL}{64\pi\sigma r^2}\Big/\frac{dT}{dr}. \tag{3}$$

In the optically thin limit (i.e. in the outermost part of the collapsing cloud), the radiation field approaches that of a point source of luminosity L at distance r. In the case of a grey opacity obeying Kirchhoff's law, the temperature in the optically thin region is independent of the opacity and is given by

$$T^4 = \frac{L}{16\pi\sigma r^2}. \tag{4}$$

A simple approximation to the temperature distribution throughout the cloud can now be constructed by adding together expressions (3) and (4). The formula thus obtained is not yet quite satisfactory, however, since it can lead to unrealistically low temperatures (i.e. $<10\,^{\circ}\mathrm{K}$) near the outer boundary of the cloud. In order to avoid this, we have assumed that the protostar is immersed in a blackbody radiation field whose temperature T_0 is equal to the initial temperature of the protostellar cloud. (Such a radiation field would in fact be present if the protostar is surrounded by an optically thick medium with temperature T_0). This introduces an additive term of T_0^4 into the expression for T^4. We then obtain

$$T^4 = -\frac{3\kappa\rho TL}{64\pi\sigma r^2}\Big/\frac{dT}{dr} + \frac{L}{16\pi\sigma r^2} + T_0^4. \tag{5}$$

This equation can be rewritten as an expression for L, analogous to the diffusion equation (2):

$$L = -\frac{64\pi\sigma r^2(T^4 - T_0^4)}{3\kappa\rho T}\frac{dT}{dr}\left[1 - \frac{4}{3}\frac{dT}{\kappa\rho T\,dr}\right]^{-1}. \tag{6}$$

Substituting this in place of equation (2), the dynamical calculations can now be carried out exactly as before.

It will be seen in Section 4 that the temperatures calculated using equation (6) agree within a factor of 2 with a probably more accurate approximation calculated as in Paper II for a non-grey opacity law. Thus the present procedure, while still crude, should at least yield reasonably realistic temperatures throughout the infalling cloud. It was shown by Larson & Starrfield (1971) that radiative heating of the infalling cloud is probably not of major importance for the dynamics of the collapse for protostellar masses less than $\sim 10\,M_\odot$; thus there should probably not be any large errors in the present calculations, although the error might become more serious for larger masses. Other effects investigated by Larson & Starrfield (1971) but not incorporated in the present calculations, such as the effects of radiation pressure and ionization on the infalling matter, become important only for masses $\gtrsim 20\,M_\odot$ and therefore should not be important in the present models (except perhaps near the end of the accretion process; see Section 6(f)).

4. RESULTS

Collapse calculations have been made for protostellar masses of 0·25, 0·5 1·0, 1·5, 2·0, 3·0, 5·0 and 10 solar masses. An initial temperature of 10°K was assumed for all masses up to 5 $M_\odot$; for a second 5 $M_\odot$ calculation and for the 10 $M_\odot$ calculation an initial temperature of 20°K was assumed, since somewhat higher temperatures may be appropriate at the lower initial densities of the more massive protostars (cf. also Larson & Starrfield 1971, where an initial temperature of 20°K was adopted for massive protostars). In each case the radius and density of the cloud have been obtained from equation (1) with

$$\mathscr{R} = 3{\cdot}36 \times 10^7 \text{ erg g}^{-1} \text{ °K}^{-1},$$

as in Paper I. (This value of $\mathscr{R}$ is based on an assumed composition of 65 per cent molecular hydrogen, 32 per cent helium, and 3 per cent heavier elements.) The initial properties of the protostellar cloud, including its radius, density, and free fall time, are tabulated for each case in Table I.

TABLE I

Initial properties of the protostellar cloud

$M/M_\odot$	T_0(°K)	R (cm)	ρ_0 (g cm^{-3})	t_f (yr)
0·25	10	4·1 (+16)	1·8 (−18)	5·0 (+4)
0·5	10	8·2 (+16)	4·4 (−19)	1·0 (+5)
1·0	10	1·6 (+17)	1·1 (−19)	2·0 (+5)
1·5	10	2·4 (+17)	4·9 (−20)	3·0 (+5)
2·0	10	3·3 (+17)	2·8 (−20)	4·0 (+5)
3·0	10	4·9 (+17)	1·2 (−20)	6·0 (+5)
5·0(a)	10	8·2 (+17)	4·4 (−21)	1·0 (+6)
5·0(b)	20	4·1 (+17)	3·5 (−20)	3·6 (+5)
10·0	20	8·2 (+17)	8·8 (−21)	7·1 (+5)

(a) *Evolution of the stellar core*

In all cases, the phases of evolution leading to the formation of a stellar core proceed in much the same way as was found in Paper I (Case 1); these include the rapid central condensation of the cloud, the formation of an opaque core in hydrostatic equilibrium, the central collapse of the core due to the dissociation of H_2 molecules, and the formation of a second, 'stellar' core of mass $\sim 10^{-3}$ $M_\odot$ when the central density reaches stellar values. In the cases with an initial temperature of 10°K, this similarity continues through the early evolution of the stellar core, including the initial adiabatic expansion and radiative cooling and contraction phases, until $\gtrsim 1/10$ of the total mass has been accreted on the core, after which the results for different masses begin to diverge. For a protostar of mass 1 $M_\odot$ the evolution follows rather closely that found in Paper I through the phase of high surface temperature and luminosity caused by infall of matter into the shock front at the surface of the core, and the final result is a star near the lower end of its Hayashi track with a radius and luminosity of about 2·1 $R_\odot$ and 1·5 $L_\odot$ respectively, compared with the 2·0 $R_\odot$ and 1·3 $L_\odot$ found in Paper I. The small difference in these results shows that the present more accurate treatment of radiative transfer in the infalling cloud has, as anticipated, not made much difference to the dynamics of the collapse or to the properties of the resulting star.

Of more interest is the comparison between the results for protostars of different masses. The evolution of the stellar core in an HR diagram is shown for all cases in Figs 1–9. In each case the dashed section of the curve represents, as in Paper I, the brief initial phase of evolution when all of the radiation emitted from the stellar core is completely reabsorbed by the material falling into the core; the beginning of the solid curve represents the point where 90 per cent of the energy radiated from the core begins to escape from the protostar as infra-red radiation. The solid dot on each of the curves indicates the point where half of the total mass has been accreted on the core. The open circle represents, for masses $<3M_\odot$, the point where essentially all of the mass has been accreted and the visual optical depth of the remnant cloud has dropped to approximately unity; for masses $\geqslant 3\,M_\odot$, the open circle represents the point where the stellar core first evolves on to the main sequence. (Optical depths have been estimated on the assumption that the visual opacity due to dust grains is 250 $cm^2\,g^{-1}$ and that the grains evaporate at a temperature of 2000°K; for present purposes, these assumptions are not critical.) The final dotted sections of the curves have not been computed but are estimated on the basis of the pre-main sequence evolutionary tracks of Iben (1965).

We see from Figs 1–4 that during the phase when the central embryo star is still accreting mass from the surrounding infalling cloud, its evolution is qualitatively the same for all masses $\lesssim 1{\cdot}5\,M_\odot$; the main difference is that the maximum surface temperature and luminosity achieved by the core increase with increasing mass. The properties of the resulting star, as shown by the open circles in Figs 1–4 and tabulated in Table II(a), also vary systematically but slowly with mass; the effective temperature and luminosity increase with mass, but the radius varies relatively little and is close to $2\,R_\odot$ for all masses $\lesssim 1\,M_\odot$. For masses less than $\sim 1{\cdot}5\,M_\odot$ the resulting star has a sizeable outer convection zone, and it first appears near the lower end of its 'Hayashi track' (Hayashi, Hoshi & Sugimoto 1962). For a mass of $1{\cdot}5\,M_\odot$ the star first appears at the bottom of its Hayashi track, and the 'Hayashi' phase is almost non-existent; for masses much greater than $1{\cdot}5\,M_\odot$, the entropy and radius of the stellar core never become large enough for a normal Hayashi phase to exist at all.

The $2\,M_\odot$ calculation (Fig. 5) represents a transition case between the low mass protostars and those of higher mass, whose pre-main sequence evolution is somewhat different. During most of the accretion process, the evolution of the $2\,M_\odot$ protostar is qualitatively similar to that of the less massive protostars. After about $1{\cdot}2\times 10^6$ yr, however, by which time nearly all of the mass has been accreted on the core but the infalling cloud still has a mass of $0{\cdot}006\,M_\odot$ and an optical depth of about 3, radiative energy transfer becomes important in the hot ($\sim 9\times 10^6$°K) inner part of the core and begins to transport a significant amount of energy to the outer layers of the core. These outer layers then increase in entropy and expand, allowing radiative energy transport to become important at greater distances from the centre; thus a 'luminosity wave' travels outward through the core. As it approaches the surface of the core, the outer layers expand on a time scale comparable with the thermal relaxation time, which becomes quite short (~ 1 day) near the surface. The core also brightens rapidly, and the luminosity increases by nearly a factor of 2 (from $15\,L_\odot$ to $26\,L_\odot$) within a period of about 4 days. After this the star settles into radiative equilibrium and evolves towards the main sequence along a 'radiative' track with decreasing radius and increasing luminosity. The optical depth of the remnant infalling cloud finally drops below

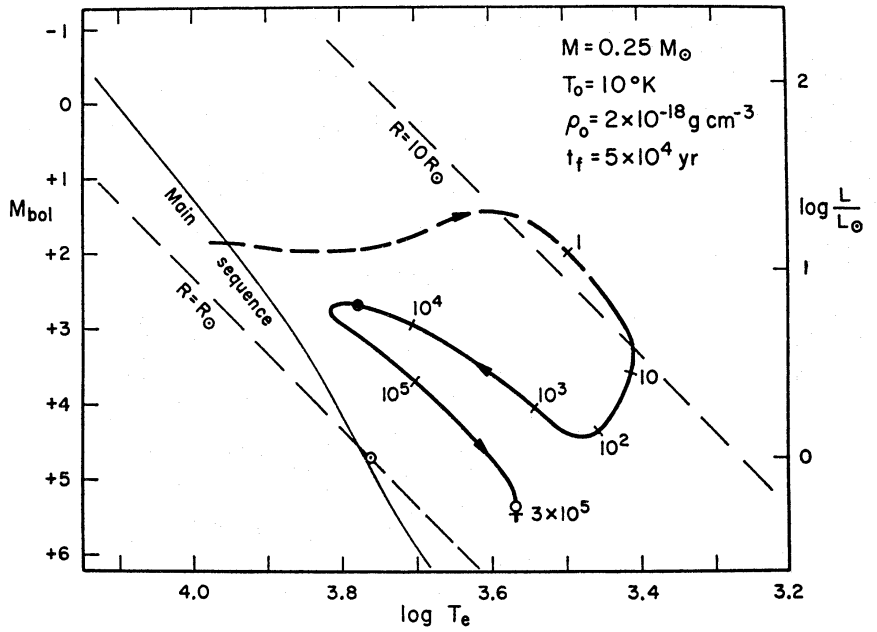

FIG. 1. *The evolution of the stellar core in the HR diagram for a protostar of* 0·25 $M_\odot$. *The time in years since the formation of the core is marked along the curve. The solid dot represents the point where half of the total mass has been accreted on the core, and the open circle represents the point where essentially all of the mass has been accreted and the stellar core becomes visible as a pre-main sequence star.*

unity during this phase of evolution, about $1{\cdot}4 \times 10^6$ yr after the formation of the core.

The protostars with masses greater than 2 $M_\odot$ (Figs 6–9) all go through a phase similar to that just described for the 2 $M_\odot$ protostar, in which a luminosity wave travels outward through the stellar core and causes a rapid expansion of the outer layers. In these cases, however, there is still a substantial amount of matter in the

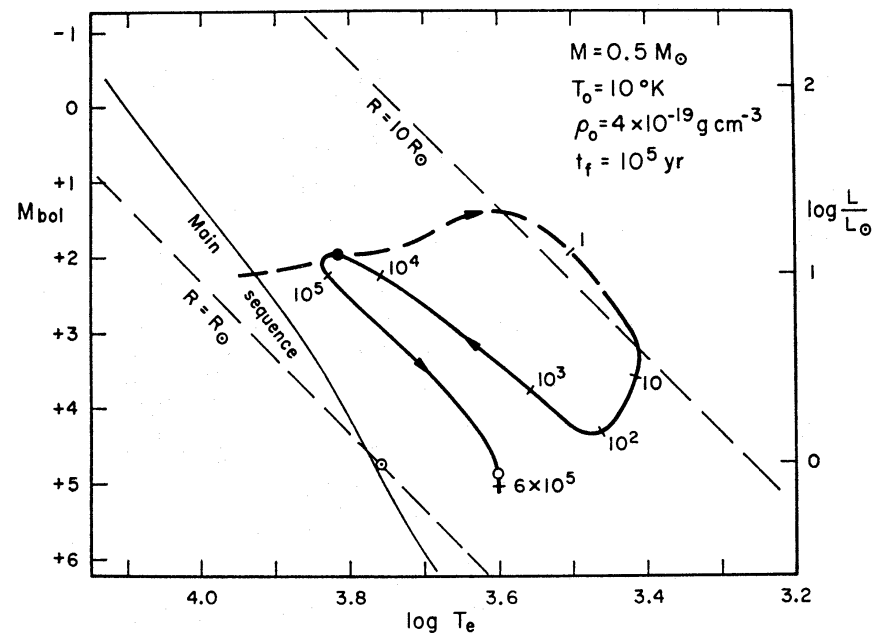

FIG. 2. *The evolution of the stellar core for a protostar of* 0·5 $M_\odot$.

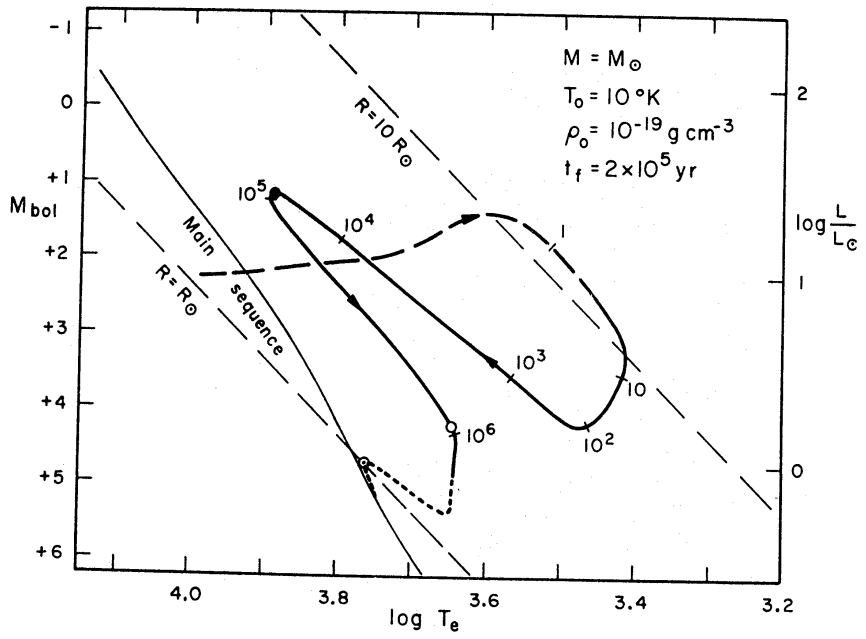

FIG. 3. *The evolution of the stellar core for a protostar of* 1·0 $M_\odot$.

infalling cloud at this time, and most of the luminosity of the protostar still comes from the kinetic energy of the material falling into the shock front at the surface of the core. Consequently, when the core expands, the infall velocity decreases and the luminosity drops. (In Fig. 6, for example, this phase begins just over 10^5 yr after the formation of the core.) When the luminosity wave reaches the surface of the core there is a rapid increase in the luminosity coming from the interior of the core, although the change in total luminosity is relatively small. For example, in the case with a total mass of 10 $M_\odot$, the luminosity coming from the interior of the core increases from about 30 $L_\odot$ to 80 $L_\odot$ over a period of about 50 days, while the total luminosity increases from 230 $L_\odot$ to 280 $L_\odot$. The mass of the stellar core

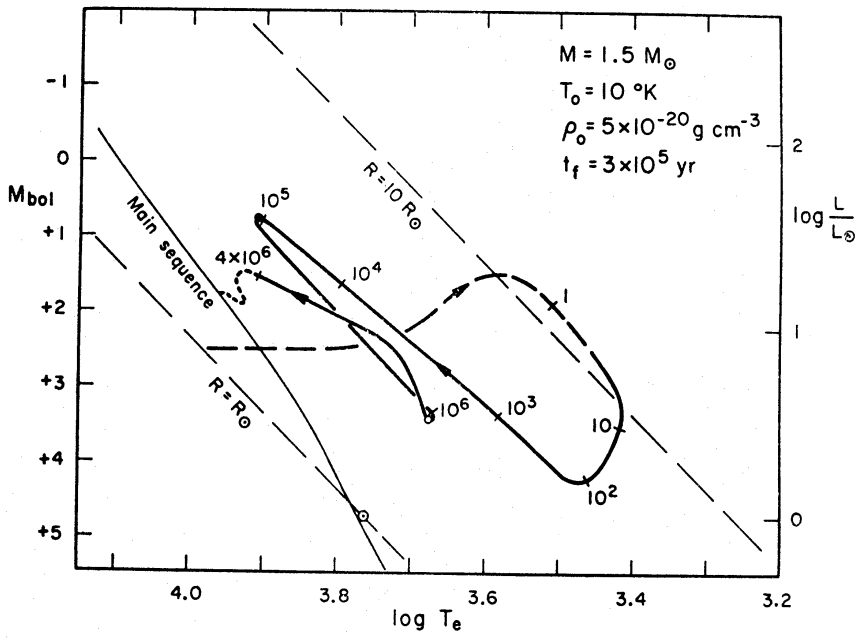

FIG. 4. *The evolution of the stellar core for a protostar of* 1·5 $M_\odot$.

at this stage is not very different in the various cases, ranging from 2·0 $M_\odot$ for a total protostellar mass of 3 $M_\odot$ to 2·8 $M_\odot$ for a total mass of 10 $M_\odot$. Once the stellar core has settled into a radiative equilibrium configuration, it once again begins to contract and evolve towards the main sequence along a radiative track. This final phase of pre-main sequence evolution still differs somewhat from previous calculations, however, in that the stellar core is still gaining mass by accretion from the surrounding cloud.

It is noteworthy that in the present calculations for protostars with masses greater than about 3 $M_\odot$, the central stellar core goes through its entire pre-main sequence evolution and becomes a main sequence star while still accreting matter

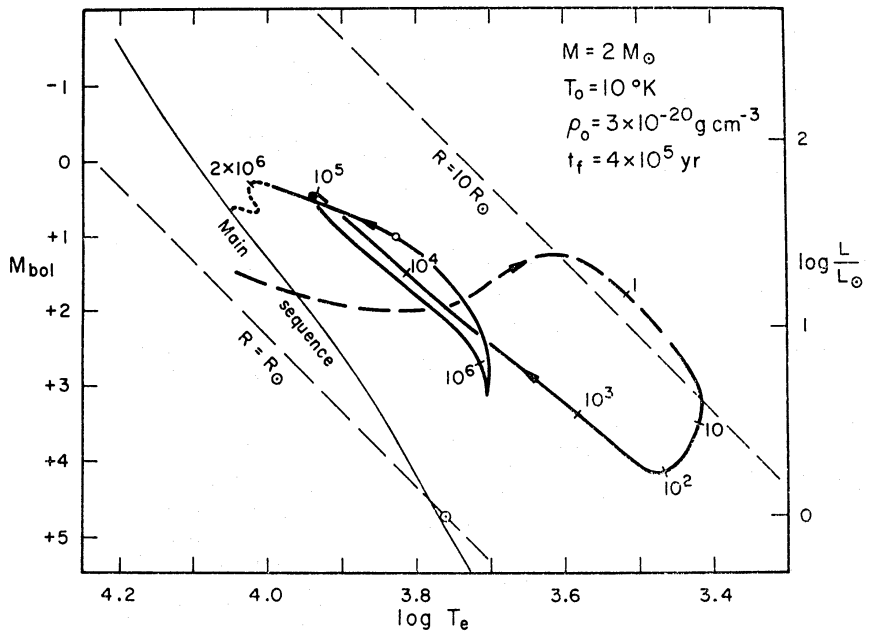

FIG. 5. *The evolution of the stellar core for a protostar of* 2·0 $M_\odot$.

from an opaque cloud of infalling material. The properties of the stellar core when it first arrives on the main sequence are tabulated in Table II(b) for protostellar masses from 3 $M_\odot$ to 10 $M_\odot$. In the case of the 3 $M_\odot$ protostar, the infalling cloud is almost exhausted by the time the central star reaches the main sequence, and has a mass of about 0·04 $M_\odot$ and an optical depth of about 3. (The optical depth could be smaller than this if the dust grains are depleted by evaporation or other effects at temperatures less than 2000°K.) For larger protostellar masses, the infalling cloud still contains a substantial amount of mass at this stage, and it heavily obscures the central star. Thus, if the present models are applicable, one would expect to see few, if any, pre-main sequence stars with masses greater than about 3 $M_\odot$, since such stars should still be obscured by dense protostellar envelopes and should not become visible until they have already reached the main sequence.

(b) *Properties of the infalling cloud*

Some results for the velocity, density and temperature distributions in the infalling cloud are shown for the 1 $M_\odot$ and 10 $M_\odot$ calculations in Figs 10 and 11 respectively. These diagrams illustrate the conditions existing in the infalling cloud

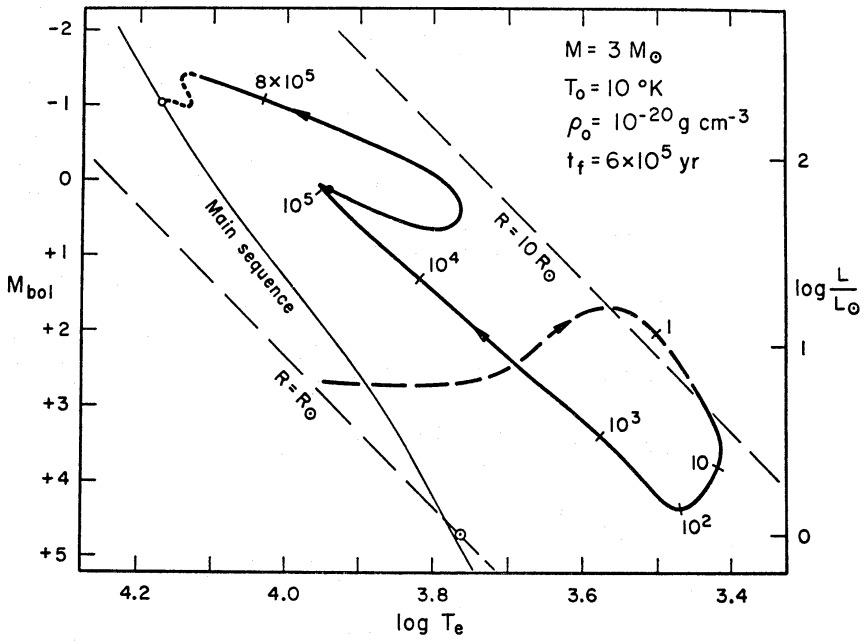

FIG. 6. *The evolution of the stellar core for a protostar of 3·0 $M_\odot$. In this and the following diagrams the open circle represents the point where the stellar core first evolves onto the main sequence, while still shrouded by its protostellar envelope.*

at the time when half of the total mass has been accreted on the stellar core. Except in the outermost part of the cloud, the velocity, density and temperature distributions are closely represented for $M = M_\odot$ by

$$u = 1{\cdot}3 \times 10^{13}\, r^{-1/2}$$
$$\rho = 1{\cdot}4 \times 10^{6}\, r^{-3/2}$$
$$T = 2{\cdot}5 \times 10^{9}\, r^{-1/2}$$

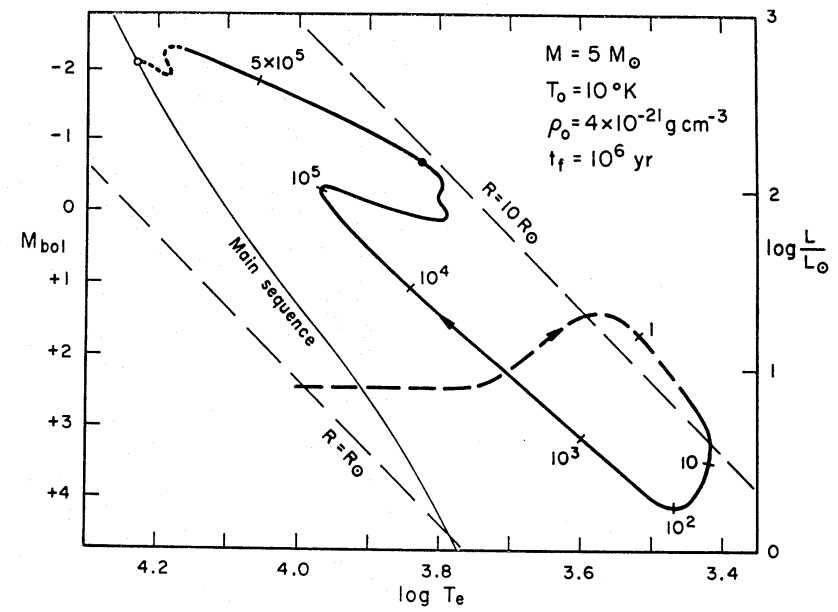

FIG. 7. *The evolution of the stellar core for a protostar of 5 $M_\odot$, case (a): initial temperature = 10°K.*

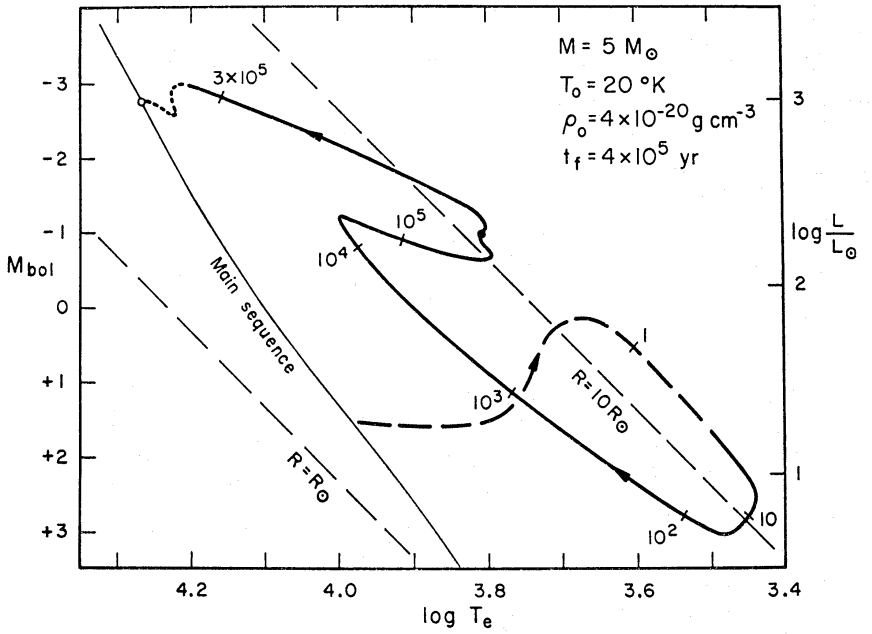

FIG. 8. *The evolution of the stellar core for a protostar of* 5 $M_\odot$, *case* (*b*): *initial temperature* = 20°*K*.

and for $M = 10\,M_\odot$ by

$$u = 4{\cdot}1 \times 10^{13}\, r^{-1/2}$$
$$\rho = 1{\cdot}4 \times 10^{6}\, r^{-3/2}$$
$$T = 7{\cdot}7 \times 10^{9}\, r^{-1/2}$$

where all quantities are in cgs units. (The fact that the density distributions are almost the same in the two cases is fortuitous, and results from the near cancellation of the effects of a factor of 10 difference in mass and a factor of 2 difference in

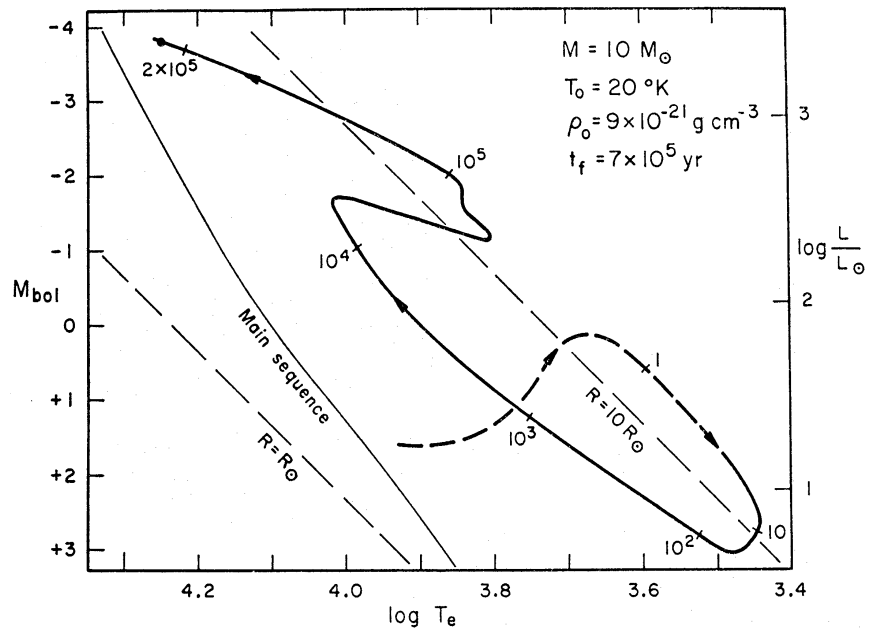

FIG. 9. *The evolution of the stellar core for a protostar of* 10 $M_\odot$.

TABLE II

(a) *Properties of newly formed stars*

$M/M_\odot$	t (yr)	log T_e	$R/R_\odot$	$L/L_\odot$
0·25	2·8 (+5)	3·57	1·8	0·55
0·5	5·0 (+5)	3·60	1·9	0·87
1·0	8·7 (+5)	3·64	2·1	1·6
1·5	1·2 (+6)	3·67	2·8	3·3
2·0	1·4 (+6)	3·83	4·0	30·0

(b) *Properties of stellar cores when they reach the main sequence*

M_{total}	M_{core}	t (yr)	log T_e	$R/R_\odot$	$L/L_\odot$
3·0	3·0	1·4 (+6)	4·17	2·2	200
5·0(a)	4·0	8·7 (+5)	4·23	2·7	520
5·0(b)	4·6	4·9 (+5)	4·27	3·1	980
10·0	5·9	3·2 (+5)	4·31	3·7	2100

initial temperature. Both density laws agree within 10 per cent with that predicted by equations (2) and (3) of Larson & Starrfield (1971).)

The dashed curves in Figs 10 and 11 represent the temperature distributions calculated by the procedure of Paper II with the non-grey opacity law

$$\kappa_\lambda = 7 \times 10^{-5} \lambda^{-3/2} \text{ cm}^2 \text{ g}^{-1}.$$

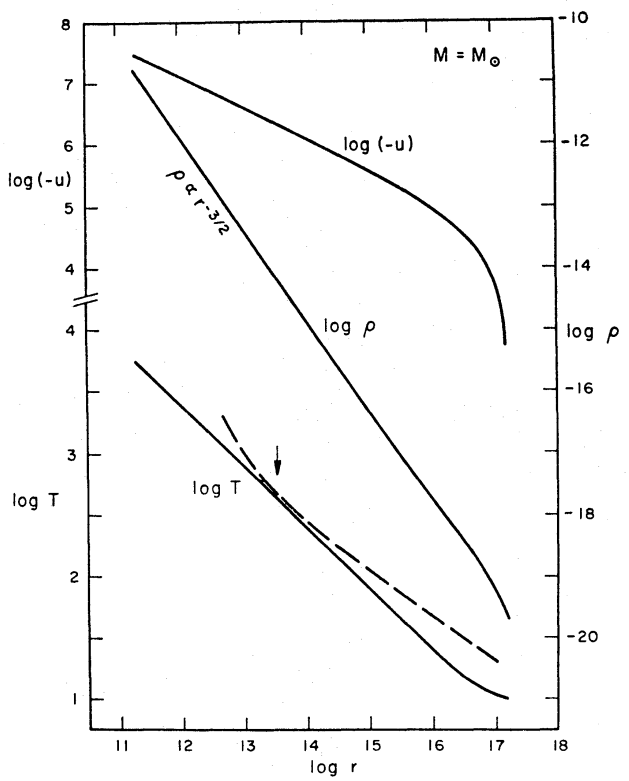

FIG. 10. *The velocity, density, and temperature distributions in the infalling envelope of a protostar of 1 $M_\odot$ at the time when half of the total mass has been accreted on the stellar core. The two temperature distributions shown refer to a grey opacity (solid curve) and a non-grey opacity (dashed curve). The arrow indicates the point where the optical depth is unity at the wavelength of peak infra-red emission.*

Since this assumption for the dust opacity, while still uncertain, is probably more realistic than the grey opacity used in the dynamical calculations, the dashed curves are probably a better approximation to the true temperature distribution. The uncertainty in temperature can be judged by comparing the solid and dashed curves; we see that they differ at most by about a factor of 2, and that the agreement is better than this over most of the range in log r. The arrow in each diagram indicates the point where the optical depth of the infalling cloud is unity at the wavelength of peak infra-red emission; we see that the two estimates for the temperature distribution are in good agreement at this point.

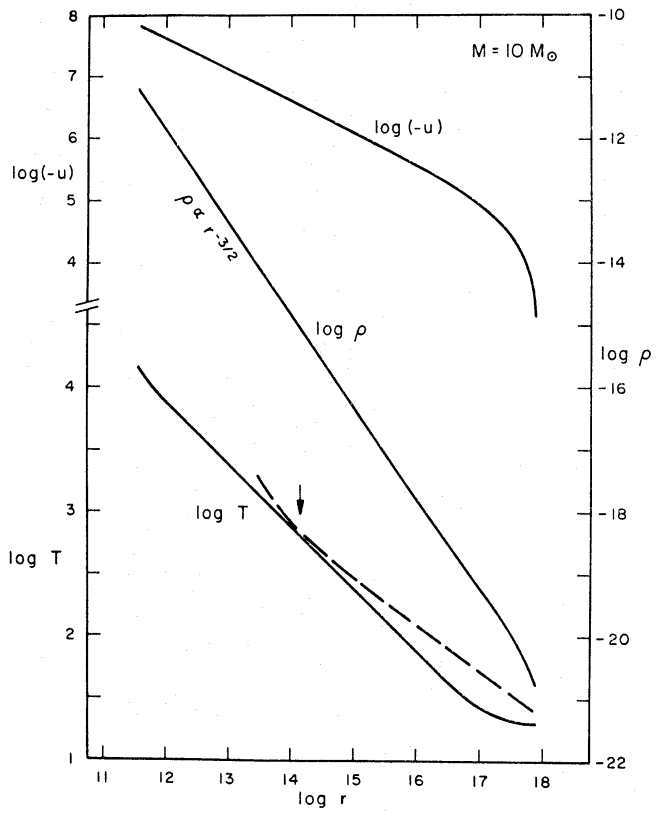

FIG. 11. *The velocity, density, and temperature distributions in the infalling envelope of a protostar of* 10 $M_\odot$ *at the time when half of the total mass has been accreted on the stellar core.*

(c) *The infra-red appearance of protostars*

Using the method and assumptions of Paper II, the wavelength of peak infra-red emission has been computed as a function of time for most of the present protostar models during the opaque phase of evolution when the protostar is visible only or primarily as an infra-red object. This allows the evolution of the protostar to be plotted in an infra-red HR diagram; the results are illustrated in Fig. 12, which shows log $(L/L_\odot)$ plotted *vs.* log λ_m, λ_m being the wavelength in microns of the peak infra-red emission (per unit wavelength interval). A scale has also been added showing the ' apparent blackbody temperature ' T_b, defined as the temperature of a blackbody with peak emission at wavelength λ_m. As was shown in Paper II, both the shape of the infra-red spectrum and the value of λ_m are sensitive to the poorly known infra-red opacity of the dust grains, so that the curves shown in Fig. 12 should be considered as only qualitatively correct.

It is evident from the dashed isochrones in Fig. 12 that the time scale for evolution increases steadily from right to left across the diagram; consequently, we would expect most observed protostars to have relatively high apparent temperatures of the order of 500–1000°K, whereas objects with temperatures of 100°K or less should be comparatively rare. Also, since observational detectability favours the brightest objects, one would expect the observed protostars to be found mostly in the upper left part of the diagram; this is in fact where most of the infra-

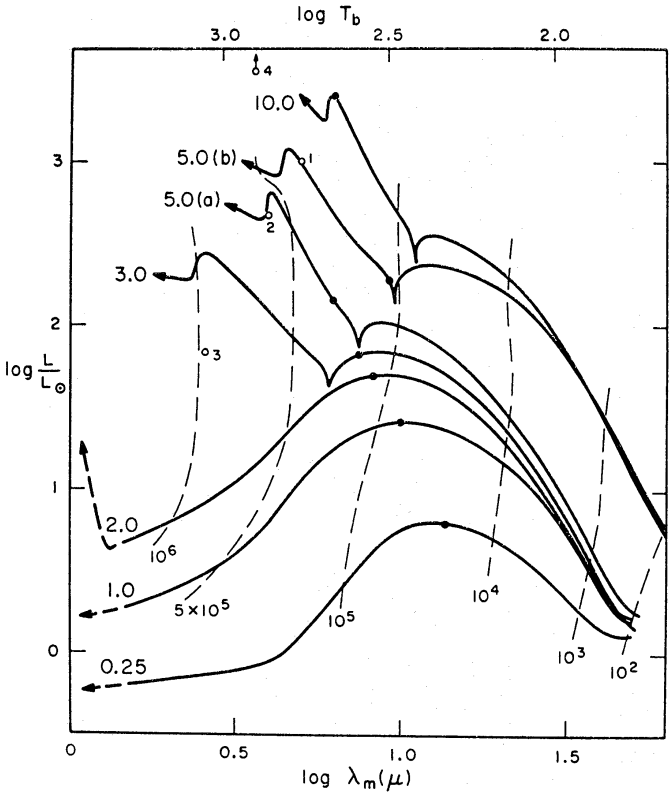

FIG. 12. *Evolutionary tracks showing the variation of the observable properties of protostars in an infra-red HR diagram. Here λ_m is the wavelength (in microns) of maximum infra-red emission and T_b is the temperature of a blackbody whose spectrum peaks at wavelength λ_m. Most of the computed cases are shown; the mass is marked near the left end of each track. The dashed lines are isochrones, with corresponding times in years marked at the bottom. The infra-red objects plotted as open circles are:* 1, *the Becklin–Neugebauer object;* 2, *R Mon;* 3, *R CrA;* 4, *LkHα* 101.

red objects currently thought to be protostars are located (see Section 6(b)). The downturn in luminosity near the end of the track for masses $\geqslant 3\,M_\odot$ occurs when the stellar core evolves onto the main sequence, and the end of the plotted curve roughly represents the point where the core becomes a main sequence star. We note that, according to the present models, for protostars appearing in the upper left part of Fig. 12 the stellar core has already evolved almost to the main sequence and may even be a main sequence star. In such cases the protostar will continue its evolution as an infra-red object whose energy is supplied by a main sequence star which is still growing in mass; this phase has not been calculated, however, since the present computer program does not incorporate nuclear energy sources.

The spectrum of a protostar during its final stages of evolution depends, among other things, on the temperature at which the dust grains evaporate. When the

amount of material remaining in the infalling cloud becomes so small that the infra-red optical depth at the point where the grains evaporate becomes equal to unity or less, the infra-red spectrum approaches a limiting form whose apparent blackbody temperature is approximately the same as the dust evaporation temperature. We have assumed that the grains evaporate at a temperature of 2000°K (appropriate for graphite grains), and accordingly the solid curves in Fig. 12 have been terminated at $T_b = 2000$°K. If the grains evaporate at a lower temperature, the curves should be terminated at a lower T_b (higher λ_m). At this stage the visual optical depth of the cloud may still be ~ 5 or higher, but it continues to decrease with continuing depletion of the protostellar cloud; eventually the central stellar object begins to shine through, and the spectrum of the protostar will then contain both a visual and an infra-red component. During this phase, the spectrum can assume a wide range of possible forms, depending on the amount and distribution of circumstellar matter, the dust evaporation temperature, etc.; a few examples are illustrated in Fig. 6 of Paper II.

5. ERRORS AND UNCERTAINTIES IN THE PRESENT MODELS

As in Paper I, purely numerical errors resulting from the coarseness of the space and time grids are believed not to exceed ≈ 20 per cent in most quantities; errors of up to ≈ 50 per cent may be present in a few places, but they are not expected to affect the results in any important way. The main sources of uncertainty in the present results lie rather in the various assumptions and simplifications which have been made, including (1) the assumed initial and boundary conditions, (2) the neglect of rotation and magnetic fields, and (3) to a lesser extent, the assumed opacities and the approximations made in treating radiative transfer problems.

With regard to the initial conditions, the first uncertain quantity is the initial temperature of a collapsing protostar. As was seen in Section 1, a temperature of the order of 10°K is thought to be typical, but variations by at least a factor of 2 about this value are quite possible. For a protostar of fixed mass, a factor of 2 change in temperature corresponds to a factor of 2 in radius, a factor of 8 in density, and a factor of 2·8 in the collapse time, assuming that the Jeans criterion is always satisfied. A further source of uncertainty arises from the Jeans criterion itself; while it is likely to be valid in an order-of-magnitude sense, deviations from it by factors of 2 or 3 in individual cases would not be surprising. If we suppose that, for one reason or another, the radius of the protostellar cloud is a factor of 2 smaller than we have assumed, the collapse time is reduced by a factor of 2·8, causing the stellar core to be unveiled at an earlier stage in its pre-main sequence evolution. From the results of Paper I we estimate that for masses near $1 M_\odot$ the effect would be to increase the radius of the resulting star by about 40 per cent and its luminosity by about a factor of 2. Thus uncertainties or variations in the initial conditions can lead to a significant dispersion in the final results.

Uncertainties in the boundary conditions can also lead to an uncertainty or scatter in the results which is probably at least comparable with that arising from the initial conditions. It is difficult to specify the boundary conditions precisely, since they depend on the interaction between a protostar and the surrounding medium. It is not even certain that a 'boundary' can be clearly defined for a collapsing protostar; it is conceivable, for example, that a protostar may continue to accrete material that initially was not part of the same protostellar condensation,

and thus end up with a mass larger than would be indicated by the Jeans criterion. Thus the present models may apply best to the more isolated protostars. Some idea of the effect of uncertainties in the initial and boundary conditions may be obtained by comparing the present 2 $M_\odot$ calculation with that described in Paper I (Case 6), which used rather different initial and boundary conditions. It seems reasonable to conclude that the radius of a newly formed star is probably not predictable to better than a factor of 2, nor its luminosity to better than a factor of 4.

Other important uncertainties, whose effects cannot yet be reliably estimated, are introduced by the two classical bugaboos in the theory of star formation, i.e. the effects of rotation and magnetic fields. The effects of magnetic fields have not yet been examined quantitatively in connection with realistic models of collapsing clouds; it seems at least possible, however, that the degree of ionization may be so low in the dense, cold, dark clouds in which stars form that magnetic effects may not be of major importance. The presence of rotation, on the other hand, will undoubtedly have an important effect on the collapse; nevertheless, as suggested in Section 1, the formation and evolution of an embryo star in a rotating cloud may proceed in a fashion qualitatively similar to what we have found for the spherical case, the principal difference being that instead of a single object, several embryo stars orbiting around each other are formed. The further development of such embryo stars remains to be determined, but the principal results may be similar in order of magnitude to those found for the spherical case. If so, the uncertainties introduced by the effects of rotation may not be much greater than those already discussed above.

With regard to radiative transfer problems, we have already noted that the temperatures in the infalling cloud may be in error by up to a factor of 2 owing to uncertainties in the dust opacity and to the approximate method used to treat radiative transfer in the infalling cloud. This does not appear to be a very important source of error for the dynamics, and is almost certainly less important than the other effects discussed above. The emitted spectrum of a protostar is, however, sensitive to the dust opacity and to the temperature distribution in the infalling cloud; also, the geometry of the dust distribution is important, and deviations from spherical symmetry can significantly alter the spectral appearance of a protostar. Thus the appearance of a protostar is probably predictable only in a qualitative sense.

Another radiative transfer problem which is only crudely treated in the present calculations is that of the transfer of radiation in the immediate vicinity of the shock front bounding the stellar core. The approximate procedure described in Paper I (Appendices A and B) for treating the shock front as a discontinuity in the flow variables can lead to a maximum error of 28 per cent in the temperature inside the shock front; this can make a noticeable but not a large difference to the evolution of the stellar core. A further error which is more difficult to evaluate can arise in the thin layer just outside the shock front during the transition from optically thick to optically thin conditions. However, this error should make no significant difference to the final results, since the transition phase is of brief duration and occurs very early in the history of the core ($\sim$ 1 yr after its formation); as may be seen by comparing Cases 1 and 4 of Paper I, the later evolution of the stellar core is practically independent of its very early history.

The calculations of Paper I have been criticized by Hayashi (1970) on the

grounds that they have neglected the reabsorption of radiation by optically thick infalling material outside the shock front. This criticism is incorrect, since radiative transfer in optically thick regions has been correctly represented by the diffusion equation, both in Paper I and in the present work. In any case, the layers just outside the shock front become optically thin only ~ 1 yr after the formation of the core, after which time radiation escapes freely from the shock front and is absorbed only by the dust grains farther out in the infalling cloud. The calculations could, however, be in error for another reason; it is conceivable that the opacities just outside the shock front may have been considerably underestimated, causing radiative energy losses from the shock front to become important at too early a stage in the calculations. This is possible because the opacity in the relevant temperature range ($2000° \lesssim T \lesssim 2500°$K) is quite uncertain, owing to the uncertain contribution from molecules.

To check out this possibility, the calculations have been repeated with the opacity artificially increased by a factor of 10 at all points outside the shock front. The radius of the stellar core then increases to a maximum value of $\sim 17\ R_\odot$ about 1·5 yr after its formation, compared with the previously obtained maximum of $12\ R_\odot$ after 1·1 yr. At this point radiative energy losses again become important, and the core begins to contract; after ~ 10 yr (still a very early stage), its evolution becomes almost identical to that previously calculated. As a more extreme example, a second test calculation was run with the assumption that the opacity outside the shock front never drops below 0·15 cm^2 g^{-1}, the assumed infra-red opacity of the dust grains. In this case the core reaches a maximum radius of $21\ R_\odot$ after 3·5 yr, but thereafter radiative energy losses once again become important, and the evolution converges toward the previous result; the radius of the resulting star, for example, is an insignificant 2 per cent larger than the $2{\cdot}1\ R_\odot$ previously obtained. Thus it appears that neither the crude treatment of radiative transfer problems nor any reasonable error in the assumed opacities can lead to large errors in the final results.

6. COMPARISON WITH OBSERVATIONS

(a) *Dark globules*

The properties of some typical dark globules have been tabulated and discussed by Bok, Cordwell & Cromwell (1971). Many of these globules are located in or near regions of active star formation, and as Bok *et al.* point out, it seems difficult to escape the conclusion that at least some of them must represent pre-stellar objects. This conclusion is strengthened by the fact that the globules are often noticeably centrally condensed; the most likely interpretation of this is that self gravitation has caused the globules to begin to condense centrally, as predicted by theoretical collapse calculations such as the present ones. The properties assumed for the initial protostellar clouds in the present calculations are remarkably similar to those of some of the dark globules described by Bok *et al.* (1971). One of the globules in NGC 2244, for example, has an estimated mass of $0{\cdot}8\ M_\odot$ and a radius of 0·06 pc; these values compare closely with the mass of $1{\cdot}0\ M_\odot$ and radius of 0·05 pc assumed for one of the present protostar models. Even allowing that the estimated globule masses are probably uncertain by at least a factor of 2, the agreement in properties between the observed globules and the theoretical protostar models is striking, and gives us some confidence in the relevance of the initial

conditions assumed in the present model calculations. In particular, the relevance of the Jeans criterion (or, equivalently, the virial theorem) appears to be confirmed, at least for the globules mentioned above.

(b) *Infra-red objects*

During a good part of its evolution, the stellar core at the centre of a collapsing protostar is completely obscured by the dense envelope of infalling material around it, and the protostar is visible only as an infra-red object. The duration of this opaque phase of evolution is of the same order as the free fall time of the initial cloud, and varies from about 3×10^5 to 10^6 yr for the present models. Because of the shortness of this time scale, one would probably not expect to observe large numbers of such objects, particularly if only the brightest ones are detectable. Nevertheless, a number of infra-red objects have been observed which appear likely to be protostars. We discuss here only the best studied infra-red objects, i.e. the ones in Orion.

In Paper II we have already discussed the Becklin–Neugebauer (1967) point source in Orion and shown that it can be interpreted as a protostar with a mass of $\sim 5\,M_\odot$. The theoretical spectra computed in Paper II provide a fairly good representation of the observed spectrum of this object, including the fact that the spectrum falls off more steeply at short wavelengths than a blackbody spectrum. Although the present evolutionary tracks for infra-red protostars (Fig. 12) are somewhat different from those of Paper II, they provide equally well for the interpretation of the Becklin–Neugebauer object as a protostar with a mass of $\sim 5\,M_\odot$ (see Fig. 12, object 1). At least one additional similar but fainter object has also been found in the same vicinity (Neugebauer, Becklin & Hyland 1971), and it may be a protostar of lower mass.

In addition to the infra-red point sources in Orion, there is also an extended infra-red nebula which is cooler but much more luminous than the point sources (Kleinmann & Low 1967; Low 1971). The B–N object appears superimposed peripherally on the K–L nebula, and may be associated with it. According to Low (1971), the K–L nebula has a mass of $\sim 200\,M_\odot$, a radius of $\sim 0{\cdot}15$ pc, and a luminosity of $\sim 10^5\,L_\odot$, although these numbers are still rather uncertain. The mass and luminosity of this object put it well outside the range of the present calculations, but it seems likely that it is an object of the same type that we have discussed, i.e. a massive protostar (or perhaps a ' proto-Trapezium ') whose energy output is supplied by a massive newly formed star or group of stars at the centre of the cloud. If so, the present calculations strongly suggest that the central star is a main sequence star which is still gaining mass by accretion; the total luminosity of $\sim 10^5\,L_\odot$ could be supplied, for example, by a single main sequence star with a mass of $\sim 27\,M_\odot$ and a spectral type of about O7. If the star is still accreting material, the density of the infalling matter can easily be high enough to prevent an H II region from forming around it until it has become even more massive and luminous (Larson & Starrfield 1971).

Penston, Allen & Hyland (1971) have suggested that the B–N object may be the highly reddened star responsible for heating the K–L nebula. If the energizing star is a main sequence O star as suggested above, and if it radiates like a blackbody in the infra-red, then it would appear at least 500 times fainter than the B–N object at wavelengths near 5 μ; therefore it cannot be identified with the B–N object. If the infra-red brightness of the energizing star is to be consistent with that of the

B–N object, the star must have a late spectral type ($\sim$Ko or later), but this may conflict with the absence of molecular absorption features in the spectrum (Penston *et al.* 1971). There is also the problem that the age of a post-main sequence star of this luminosity would be $\sim 5 \times 10^6$ yr, whereas the free fall time in the K–L nebula is only about 10^5 yr; it is difficult to see how such a cloud could have remained around the star for so long, and equally difficult to see how it could have recently formed around such a luminous star. If instead one imagines that the energizing star is a pre-main sequence supergiant, its age would be only $\approx 10^3$ yr, and it could have formed only in an exceedingly dense cloud whose free fall time does not exceed $\sim 10^3$ yr; this seems implausible, and may conflict with the observations. Thus it seems likely that the B–N object is not the highly reddened star responsible for energizing the K–L nebula, but is instead a separate (although possibly associated) protostar of much smaller mass.

(c) *Stars with strong infra-red emission*

After most of the protostellar envelope has been accreted on the core or otherwise dissipated, the optical depth of the infalling cloud becomes small enough to allow visual radiation from the stellar core to escape, perhaps with considerable scattering from dust grains. The spectrum of the protostar will then show two components—a stellar spectrum, perhaps still strongly influenced by circumstellar matter, and an infra-red spectrum similar to that of an opaque protostar. Most of the known stars with strong infra-red emission are not protostars, but there are a number of objects whose properties appear to be best explained by interpreting them as protostars or newly formed stars. Examples of this class of object are R Mon, R CrA, V380 Ori, LkHα 101 and Z CMa (Herbig 1956, 1960; Mendoza 1970; Low *et al.* 1970; Neugebauer *et al.* 1971; Cohen & Woolf 1971). All of these stars are embedded in small, dense clouds of reflection and/or absorption nebulosity, and all are located in or near regions of active star formation; this circumstantial evidence makes it seem very likely that they are very young newly formed stars.

The best studied object of this type, R Mon, has an infra-red spectrum which is similar to that of the Becklin–Neugebauer object, and it is fairly well represented by the theoretical spectra computed in Paper II for opaque protostars (Neugebauer *et al.* 1971). R Mon is plotted in the infra-red HR diagram of Fig. 12 (object 2), and from its position in this diagram we see that it can be interpreted as a protostar with a mass of ~ 4 or $5\ M_\odot$. If the present models are applicable, they would imply that the protostellar envelope of R Mon has a mass of $\sim 1\ M_\odot$ and that the central star has a mass of $\sim 3{\cdot}5\ M_\odot$ and an effective temperature of the order of $1{\cdot}5 \times 10^4$°K. These predictions are difficult to compare with the observations, since R Mon does not show a normal stellar spectrum; according to Herbig (1968), all of the observed spectral features may originate in a circumstellar shell. Nevertheless, temperatures of the order of 10^4°K appear to be indicated by the appearance of strong Balmer absorption lines in the spectrum.

R CrA is another object which is similar in many respect to R Mon, except that it is fainter and has an infra-red spectrum which peaks at a shorter wavelength (Fig. 12, object 3). Comparing with the present models, we find that R CrA can be interpreted as a protostar with a total mass of $\sim 2{\cdot}5\ M_\odot$, nearly all of which is in the central star. LkHα 101 is another object associated with dense nebulosity, and it has an infra-red spectrum similar to that of the Becklin–Neugebauer object; however, it has a much higher luminosity of $\sim 2{\cdot}5 \times 10^4\ L_\odot$ (Cohen & Woolf

1971). This luminosity is outside the range of the present calculations, but it could be supplied by a central star of mass $\sim 15\ M_\odot$. Extrapolation of the present models suggests that the central star is a main sequence star, and that it may be surrounded by a cloud of comparable mass and may still be accreting matter from it.

(d) *T Tauri stars*

Because of their close association with young stars and interstellar matter, and because of their location above the main sequence in the HR diagram, it has long been believed that the T Tauri stars are very young newly formed stars. Most of the objects mentioned above in Section 6(c) are classed as T Tauri stars, and as such they form a subgroup which we may consider 'extreme' T Tauri stars because their observed properties are still dominated by dense circumstellar clouds. Most T Tauri stars also show excess infra-red emission attributable to circumstellar shells, but in most cases the infra-red emission is not dominant. These more 'normal' T Tauri stars are thus naturally interpreted as newly formed stars whose protostellar clouds have almost disappeared.

According to Herbig (1962) most of the T Tauri stars have effective temperatures in the range $3{\cdot}50 \lesssim \log T_e \lesssim 3{\cdot}75$ and radii between $1\ R_\odot$ and $3\ R_\odot$; a typical radius is about $2\ R_\odot$. Comparing these values with the predicted effective temperatures and radii of newly formed stars as listed in Table II(a), we see that there is very good agreement between the observed properties of T Tauri stars and the predicted properties of newly formed stars with masses $\lesssim 1{\cdot}5\ M_\odot$. The scatter in the properties of T Tauri stars may have at least two possible causes, in addition to the obvious ones of differences in mass and age: (1) Differences in the initial and boundary conditions can cause a newborn star of given mass to appear at somewhat different positions in the HR diagram, as discussed in Section 5. (2) Many T Tauri stars probably have remnant shells of dusty material around them; absorption in such circumstellar shells can lead to an appreciable scatter of positions in the HR diagram. Evidence for such circumstellar matter around many pre-main sequence stars has been found by Strom, Strom & Yost (1971) and by Strom *et al.* (1972a, b).

It thus appears that the distribution of T Tauri stars in the HR diagram, including the scatter, agrees with theoretical expectations based on the present model calculations. We can even understand why there are relatively few more luminous T Tauri-like stars located far away from the main sequence; according to the present calculations, newly formed stars with masses greater than about $3\ M_\odot$ will already have evolved close to or onto the main sequence by the time the surrounding cloud has thinned out sufficiently to reveal the central star. Herbig (1960) has described a number of luminous T Tauri-like stars of spectral types B and A which are closely associated with dense circumstellar nebulosity; these are very probably newly formed stars which have just begun to shine through the surrounding nebulosity. According to Strom *et al.* (1972b), a number of these stars are indeed main sequence stars, as would be predicted by the present calculations.

Additional evidence in favour of the present picture of star formation is provided by Walker's (1972) observations of redshifted absorption lines in some T Tauri stars, which are attributable to infall of matter. The present calculations predict that the infall of the last remnants of the protostellar cloud should be observable just after the stellar core becomes visible, and should continue for

perhaps 10^5 yr or so before dying out or being overpowered by mass ejection. This suggests that the stars showing infall of matter (YY Ori stars) are among the very youngest stars, which is consistent with their positions in the HR diagram. The infall velocities of 150 to 400 km s^{-1} observed by Walker are in good agreement with the theoretical infall velocities, which vary from about 200 to 400 km s^{-1} for masses between 0·25 and 1·0 $M_\odot$. This agreement provides an independent check on the radii of the YY Ori stars and shows that they cannot much exceed 2 $R_\odot$. The fact that stars are observed to be forming by accretion at such relatively small radii and luminosities is evidence against earlier ideas that stars form at the top of the Hayashi track with much larger radii and luminosities.

(e) *HR diagrams of young clusters*

Some of the pre-main sequence stars in young clusters such as the Orion cluster and NGC 2264 are T Tauri stars, particularly among the later spectral types; thus there is clearly a continuity between the T Tauri stars and other pre-main sequence stars which do not show T Tauri characteristics and presumably represent a later stage of evolution. Consequently the above discussion concerning the positions of T Tauri stars in the HR diagram is still relevant here; one would again expect some scatter of positions in the HR diagram arising from such effects as differences in the initial conditions and differences in the amount of circumstellar absorption. Strom *et al.* (1971; 1972a, b,) and Breger (1972) have found evidence for circumstellar shells around many pre-main sequence stars and have shown that such shells can account for some of the scatter of these stars in the HR diagram. The existence of such shells is in agreement with the present prediction that the remnant protostellar envelope around a newly formed star has a lifetime of the order of 10^6 yr. Because of such effects, it is difficult to interpret the HR diagrams of very young clusters entirely in terms of the masses and ages of the stars, as is usually done; thus it is difficult to determine a precise age or age distribution for such a cluster by comparison with theoretical isochrones.

A different and perhaps better way of comparing theory and observations is to compare the positions of pre-main sequence stars in the HR diagram with the predicted positions at which newly formed stars of different masses should first appear after circumstellar absorption has become unimportant. In Fig. 13 we have taken the predicted properties of newly formed stars as listed in Table II and plotted them as open circles in a theoretical HR diagram. The heavy curve joining these points represents the approximate locus along which newly formed stars of different masses should first appear. The dashed curve represents the estimated locus along which stars would appear if the radius of the protostellar cloud were a factor of 2 smaller than we have assumed; the difference between the two curves is a minimal indication of the uncertainty that can result from uncertainties in the initial conditions, boundary conditions, etc. For reference, the pre-main sequence isochrones of Iben & Talbot (1966) are also shown; it turns out that, where comparisons can be made, the present results agree fairly well with these isochrones. It should be noted, however, that the isochrones for times $\lesssim 10^6$ yr are no longer relevant, since at such times the embryo star is still heavily shrouded by its protostellar envelope and is still accreting material from it.

We see from Fig. 13 that the predicted locus of newly formed stars in the HR diagram generally lies between the isochrones for 10^6 and 2×10^6 yr, and that the possible spread in positions of newly formed stars resulting from variations in the

initial conditions, etc., corresponds to an 'age spread' of at least 3×10^6 yr and perhaps as much as 10^7 yr. These predictions are in qualitative agreement with the distribution of pre-main sequence stars in the HR diagram for the clusters studied by Iben & Talbot (1966), even without allowing for a real age spread. In fact an age spread of the order of 10^7 yr or more is probably present and is also expected theoretically (see below), but it is difficult from the HR diagram alone to separate age differences from other effects. It is also difficult to assign a precise age to a young cluster or even to interpret differences between cluster HR diagrams in terms of age differences, since it is evident from Fig. 13 that a systematic difference

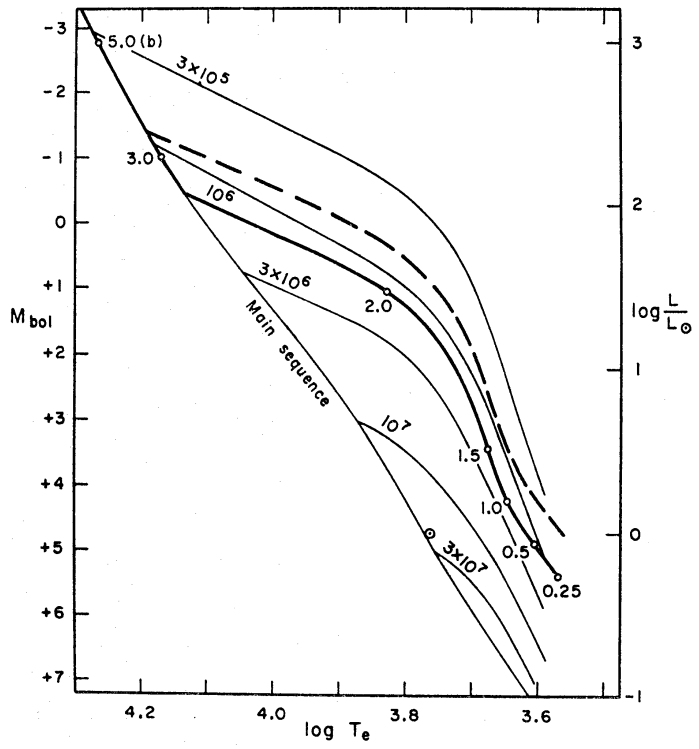

FIG. 13. *The predicted loci along which newly formed stars first appear in the HR diagram. The open circles are transferred from Figs* 1–8, *and the heavy solid curve is the locus along which stars should first appear if all of the assumptions of the present models are correct. The dashed curve shows the estimated result obtained when the initial temperature is increased from* 10°*K to* 20°*K in all cases. Isochrones from Iben & Talbot* (1966) *are also shown for reference.*

in the initial conditions can mimic an age difference of the order of 10^6 yr or more. Thus 10^6 yr is probably about the youngest cluster age or the smallest age difference between clusters that can be meaningfully determined from cluster HR diagrams.

It is of interest to consider what sort of age spread might be expected for the stars in a young cluster such as the Orion cluster. The time required for a star to form from a protostellar cloud is of the order of a few free fall times, and the variation in formation time caused by differences in the initial and boundary conditions is of the same order. From Table I we see that the free fall times for the present protostar models lie between about 10^5 and 10^6 yr, so that an age spread of at least a few times 10^6 yr is to be expected. Since the free fall time depends on the density of the protostellar cloud, we can also estimate the free fall time observationally by taking the observed density of matter (stars plus gas) in young clusters

such as the Orion cluster and assuming that this is the same as the density of the interstellar cloud from which the cluster formed. In the Orion cluster the density of matter varies from $\approx 10^{-19}$ g cm^{-3} at the centre to $\approx 10^{-22}$ g cm^{-3} in the outer regions (Menon 1966); the corresponding range of free fall times is from 2×10^5 to 6×10^6 yr. Thus an age spread of at least 10^7 yr is to be expected. An even larger age spread can occur if the cluster continues to accrete matter from a more extended concentration of interstellar matter around it; in this case the formation of the cluster may continue for a period of several times 10^7 yr. Thus the observed scatter of pre-main sequence stars in the HR diagram may plausibly be caused mostly by an age spread, although other effects will also contribute, as we have seen.

(f) *FU Ori* and *V1057 Cyg*

FU Ori and V1057 Cyg (LkHα 190) are two remarkable T Tauri-like stars which have been observed to brighten by ~ 5 mag within a year and then remain approximately constant at the higher luminosity (Herbig 1966; Herbig & Harlan 1971; Cohen & Woolf 1971). Both objects presently have luminosities of the order of $10^3 L_\odot$ (with considerable uncertainty), implying masses of the order of $5 M_\odot$. While the spectra are abnormal, they appear to indicate effective temperatures of the order of 7×10^3°K for FU Ori and 10^4°K for V1057 Cyg. These objects resemble R Mon in bolometric luminosity and in the temperature of the central stellar object; the main difference is that in R Mon most of the stellar radiation is absorbed and converted into infra-red radiation by a dense circumstellar shell, whereas this does not appear to be the case for FU Ori or V1057 Cyg (Cohen & Woolf 1971). Thus if the circumstellar envelope around R Mon were to be somehow suddenly removed, an object like FU Ori or V1057 Cyg might result. As remarked by Cohen & Woolf (1971), it is not impossible that the change in spectral appearance of V1057 Cyg could be due to the rapid disappearance of a circumstellar shell.

If the present protostar models are relevant, they appear to offer no possibility of explaining the sudden increase in luminosity by a factor of 100 or more as a result of any change in the structure of the central star. We are therefore led to regard the rapid dissipation of a circumstellar shell as the most promising possibility for explaining FU Ori and V1057 Cyg. It is consistent with this possibility that the observed time scale for brightening is comparable with the dynamical time scale for the circumstellar shell (≈ 1 yr). In the present models there are no rapid changes in the structure of the circumstellar absorbing shell, since it is continually replenished by infall or matter from the outer regions of the protostellar cloud; this infall process varies only with a time scale of $\approx 10^5$ yr. Thus if the circumstellar shell is to be permanently dissipated it is necessary that the whole accretion process must somehow be rapidly cut off.

Such a rapid cut-off of the accretion process may in fact occur as a result of the action of radiation pressure on the infalling material. First, it is clear that for a sufficiently luminous protostar radiation pressure will eventually become dominant over gravity after the infalling cloud has become optically thin. This follows from equation (12) of Larson & Starrfield (1971), according to which the ratio of radiation pressure to gravity in an optically thin region is given by

$$\left|\frac{\text{radiation pressure}}{\text{gravity}}\right| = 7{\cdot}8 \times 10^{-5}\, \kappa \frac{L/L_\odot}{M/M_\odot}. \qquad (7)$$

If we adopt $\kappa \sim 250$ cm^2 g^{-1} for the opacity of interstellar matter at visual wavelengths, we find that radiation pressure is dominant if

$$\frac{L/L_\odot}{M/M_\odot} \gtrsim 50, \tag{8}$$

which occurs for masses greater than $\sim 3\,M_\odot$. Thus for protostars more massive than this the infall of matter will eventually be halted and reversed by radiation pressure (assuming that there is always strong frictional coupling between dust grains and gas).

Since the infra-red opacity of dust grains is much smaller than the visual opacity, radiation pressure does not become important in the outer part of the protostellar cloud until the circumstellar obscuration has been lifted sufficiently to allow an appreciable amount of visual radiation to escape. This can happen if the circumstellar absorbing shell is disrupted, even temporarily, by radiation pressure acting directly on it; this will allow visual radiation to escape from the shell and halt further infall of material, so that the shell is not replenished and disappears permanently. If the central star ejects material, as T Tauri stars often do, the resulting stellar wind may have a similar effect in disrupting the circumstellar shell. The point at which radiation pressure becomes sufficient to influence the dynamics of the shell may be estimated by determining when the radiation pressure acting on the shell becomes comparable with the dynamical pressure of the infalling material in the shell (Larson & Starrfield 1971). If we consider a protostar of mass $5\,M_\odot$ and assume as before that the dust evaporates at a temperature of 2000°K, we find that radiation pressure becomes competitive with dynamical pressure when the infalling cloud has a mass of $\sim 0{\cdot}05\,M_\odot$ and a visual optical depth of ~ 6. If the shell is disrupted by an instability at this point, as seems likely, the protostar will brighten rapidly by about 6 mag on a time scale of the order of 1 yr. This predicted behaviour is in striking, if perhaps fortuitous, agreement with the observed behaviour of FU Ori and V1057 Cyg.

7. CONCLUDING REMARKS

The present protostar models have been computed using what might be called 'standard assumptions', the most important of which are (1) that the initial temperature of the protostellar cloud is of the order of 10–20°K, and (2) that the initial conditions satisfy the Jeans criterion. In addition, the models neglect any possible effects of rotation or magnetic fields. We have argued in Section 5 that the present models are probably qualitatively correct and quantitatively not in error by orders of magnitude. Ultimately, however, the correctness or relevance of the present calculations must be judged by the extent to which the theoretical predictions agree with observations. It is therefore very encouraging that the present theory appears to account qualitatively for the properties of most of the types of objects currently thought to represent protostars or newly formed stars. Even the quantitative agreement between theory and observations is remarkably good, considering the theoretical uncertainties and the idealized nature of the models. Perhaps the errors introduced by neglecting rotation, magnetic fields, etc., are less serious than might have been feared. At any rate, it would appear that the deficiencies of the present models are mostly of a quantitative nature, and that the

basic picture of star formation by non-homologous collapse leading to the formation of a central embryo star which continues to grow by accretion is almost certainly correct.

ACKNOWLEDGMENT

I thank Mme Kathlyn Auer for considerable assistance with the computations and with the preparation of diagrams.

Yale University Observatory, New Haven, Connecticut 06520

REFERENCES

Becklin, E. E. & Neugebauer, G., 1967. *Astrophys. J.*, **147,** 799.
Bodenheimer, P. & Sweigart, A., 1968. *Astrophys. J.*, **152,** 515.
Bok, B. J., Cordwell, C. S. & Cromwell, R. H., 1971. *Dark Nebulae, Globules, and Protostars*, ed. B. T. Lynds, p. 33. University of Arizona Press, Tucson.
Breger, M., 1972. *Astrophys. J.*, **171,** 539.
Cohen, M. & Woolf, N. J., 1971. *Astrophys. J.*, **169,** 543.
Field, G. B., 1970. *IAU Symposium No. 39: Interstellar Gas Dynamics*, ed. H. J. Habing, p. 51. D. Reidel, Dordrecht.
Hayashi, C., 1970. *Évolution Stellaire Avant la Séquence Principale* (16th Liège Symposium), p. 127. Université de Liège.
Hayashi, C., Hoshi, R. & Sugimoto, D., 1962. *Prog. theor. Phys. Suppl., No.* **22.**
Heiles, C., 1971. *A. Rev. Astr. Astrophys.*, **9,** 293.
Herbig, G. H., 1956. *Publ. astr. Soc. Pacific*, **68,** 353.
Herbig, G. H., 1960. *Astrophys. J. Suppl.*, **4,** 337.
Herbig, G. H., 1962. *Adv. Astr. Astrophys.*, **1,** 47.
Herbig, G. H., 1966. *Vistas in Astronomy*, **8,** 109.
Herbig, G. H., 1968. *Astrophys. J.*, **152,** 439.
Herbig, G. H. & Harlan, E. A., 1971. *Inf. Bull. Var. Stars*, No. 543.
Hummer, D. G. & Rybicki, G. B., 1971. *Mon. Not. R. astr. Soc.*, **152,** 1.
Iben, I., 1965. *Astrophys. J.*, **141,** 993.
Iben, I. & Talbot, R. J., 1966. *Astrophys. J.*, **144,** 968.
Kleinmann, D. E. & Low, F. J., 1967. *Astrophys. J. Letters*, **149,** L1.
Larson, R. B., 1969a. *Mon. Not. R. astr. Soc.*, **145,** 271 (Paper I).
Larson, R. B., 1969b. *Mon. Not. R. astr. Soc.*, **145,** 297 (Paper II).
Larson, R. B., 1972. *Mon. Not. R. astr. Soc.*, **156,** 437.
Larson, R. B. & Starrfield, S., 1971. *Astr. Astrophys.*, **13,** 190.
Low, F. J., 1971. *Dark Nebulae, Globules, and Protostars*, ed. B. T. Lynds, p. 115. Univ. of Arizona Press, Tucson.
Low, F. J., Johnson, H. L., Kleinmann, D. E., Latham, A. S. & Geisel, S. L., 1970. *Astrophys. J.*, **160,** 531.
Mendoza, E. E., 1970. *Évolution Stellaire Avant la Séquence Principale* (16th Liège Symposium), p. 319. Université de Liège.
Menon, T. K., 1966. *Trans. IAU, Vol. XII B*, ed. J. C. Pecker, p. 455. Academic Press, London & New York.
Neugebauer, G., Becklin, E. E. & Hyland, A. R., 1971. *A. Rev. Astr. Astrophys.*, **9,** 67.
Penston, M. V., Allen, D. A. & Hyland, A. R., 1971. *Astrophys. J. Letters*, **170,** L33.
Strom, K. M., Strom, S. E. & Yost, J., 1971. *Astrophys. J.*, **165,** 479.
Strom, S. E., Strom, K. M., Brooke, A. L., Bregman, J. & Yost, J., 1972a. *Astrophys. J.*, **171,** 267.
Strom, S. E., Strom, K. M., Yost, J., Carrasco, L. & Grasdalen, G., 1972b. *Astrophys. J.*, **173,** 353.
Walker, M. F., 1972. *Astrophys. J.*, to be published.